Journal of Advanced Informatics in Water, Soil, and Structure 2025 1 (1) 98-114

Journal of Advanced Informatics in Water, Soil, and Structure

journal homepage: www.wss.torbath.ac.ir

Research Article

Prediction of Compressive Strength of Fly Ash-based Geopolymer Concrete Using Artificial Neural Network Model

Mohsen Nia, E. [a*], Toufigh, V. [a]

[a] *Department of Civil Engineering, Sharif University of Technology, Tehran, Iran*

ARTICLE INFO

Received date: 28 Dec 2023
Accept date: 13 Jun 2024
Published date: 01 Jan 2025

Keywords:
Geopolymer Concrete, Fly Ash, Machine Learning, Artificial Neural Network, Compressive Strength

Abstract

Geopolymer concrete is an environmentally friendly alternative to traditional concrete, using waste materials as a cementitious material. One of the main challenges in using geopolymer concrete in the construction industry is the lack of a standard mixing design. This study presents a neural network model for predicting the compressive strength of fly ash-based geopolymer concrete. To achieve this goal, 162 architectures reported in articles published between 2000 and 2020 were collected. In this study, ten input variables (such as the water-to-solid ratio of fly ash, sodium hydroxide, and sodium silicate solution, the total ratio of sodium hydroxide and sodium silicate solution to fly ash) and one output variable (i.e. compressive strength of fly ash-based geopolymer concrete) were used. The best-presented model had R^2, RMSE (MPa), MAPE (%), and MAE (MPa) indices of 0.828, 3.56 MPa, 7.74%, and 2.91 MPa, respectively, for the test data, which indicates acceptable accuracy. Finally, by comparing this model with previous studies, the proposed model showed that it can estimate the compressive strength of fly ash-based geopolymer concrete with acceptable accuracy, which can save time and money.

Homepage: www.wss.torbath.ac.ir

*Corresponding Author:
Mohsennia, Ehsan
Email: Mohsennia.ehsan@gmail.com
ORCID: 0009-0001-4599-9204

https://doi.org/10.22048/WSS.2024.432893.1006

How to cite this article:

Mohsen Nia, E., Toufigh, V. (2025). Prediction of Compressive Strength of Fly Ash-based Geopolymer Concrete Using Artificial Neural Network Model. *Journal of Advanced Informatics in Water, Soil, and Structure*, *1*(1), 98-114.

1- Introduction

Concrete is one of the most widely used materials in the world, where Ordinary Portland Cement (OPC) is repeatedly used as the binding material (Malekian and Chitsaz, 2021; Possan et al., 2017; Siddique et al., 2011). The primary environmental issue with conventional concrete is the extensive consumption of cement in it, leading to a significant release of carbon dioxide (CO_2). Annually, 5 to 7 percent of the global CO_2 emissions are attributable to OPC production (Hendriks et al., 1998). Consequently, reducing the consumption of conventional cement in the construction industry leads to a reduction in CO_2 emissions, which can mitigate the pace of climate change (Hansen et al., 1981). One solution to reduce carbon dioxide emissions is replacing cementitious materials with cement alternatives. In this regard, Davidovits introduced geopolymer concrete as a substitute for conventional cement-based concrete (Davidovits, 1993). Geopolymeric materials typically comprise industrial by-products, natural raw materials, and agricultural waste containing significant aluminosilicates (Almutairi et al., 2021; Fallah and Nematzadeh, 2017; Gholhaki et al., 2018). Consequently, particle bonding occurs more in these materials due to the reactions of aluminosilicates. In other words, the hydration reaction that leads to the release of carbon dioxide in the production of Portland cement-based concrete does not occur in the production process of geopolymer concrete. Studies show that geopolymer concrete produces 5 to 6 times less carbon dioxide than ordinary Portland cement (McLellan et al., 2011). Additionally, this approach reduces environmental damage associated with the disposal of industrial and agricultural waste due to the use of waste materials (Shahmansouri et al., 2021).

Fly ash is one of the cementitious materials used in geopolymer concrete. Thermal power plants produce fly ash in large quantities as a by-product. Using fly ash in geopolymer concrete reduces carbon dioxide emissions and mitigates other environmental impacts by disposing of them as by-products in concrete (Olivia and Nikraz, 2011). Based on these properties, in recent decades, many researchers have investigated fly ash-based geopolymer concrete's mechanical and chemical properties and its design parameters. Recent studies have shown that this type of geopolymer concrete exhibits acceptable mechanical properties in terms of compressive strength, fire resistance, and resistance to sulfate attack. In the production of geopolymer materials, sodium silicate is often used along with another alkaline substance, such as sodium hydroxide or potassium hydroxide, to activate aluminosilicates and participate in the geopolymerization reaction (Al Bakri et al., 2012; Vora and Dave, 2013).

Research on fly ash-based geopolymer concrete (GPC) has been widely conducted in recent years due to its properties being comparable to cement and its environmental benefits (Verma et al., 2023). However, the complexity and uncertainty of design parameters have made it challenging to develop a systematic mixing scheme for geopolymer concrete. Recently, researchers have utilized statistical methods to predict the compressive strength of geopolymer concrete. For instance, in a study by Ahmed et al. (2021), the performance of linear and nonlinear multivariable regression models for predicting the compressive strength of fly ash-based geopolymer concrete with consistent input variables was compared. Their results showed that the nonlinear model exhibited less error than the linear model, indicating a nonlinear relationship between the mixing design of geopolymer concrete and its strength. Multivariate Adaptive Regression Splines (MARS) are a form of regression analysis in statistics. A non-parametric regression technique can be viewed as an extension of linear models, automatically modeling nonlinear relationships between variables. Lokuge et al. (2018) utilized this model to develop a fly ash-based geopolymer concrete mixing design. Toufigh and Jafari (2021) also predicted the compressive strength of fly ash-based geopolymer concrete using the Bayesian linear regression algorithm.

Machine learning techniques have become powerful tools for solving statistical problems in engineering challenges (Kamath et al., 2024; Khambra and Shukla, 2023; Moein et al., 2023). One of the prominent machine learning techniques is Artificial Neural Networks (ANN). Artificial Neural Networks are a powerful tool for solving regression problems and can accurately predict complex relationships between input and output variables. Nowadays, neural networks have been widely used to predict the properties of concrete (Jafari and Toufigh, 2023). Deshpande et al. (2014) utilized ANN, decision tree model, and nonlinear

regression to predict the compressive strength of concrete, with their results indicating that ANN models lead to the highest accuracy. Siddique et al. (2011) adopted ANN to estimate the 28-day compressive strength of their self-compacting concrete containing ash, resulting in highly accurate results. Bu et al. (2021) precisely predicted the compressive strength of recycled aggregate concrete using ANN. Similarly, BKA et al. (2021) employed ANN to predict the compressive strength of recycled concrete, with their research findings showing that the ANN model can provide correlation coefficients of 0.92-0.94.

Many parameters affect the compressive strength of GPC based on fly ash. Also, the relationship between these parameters is very nonlinear. It should be noted that the laboratory construction of concrete samples and checking all these parameters on the final compressive strength is a complex, time-consuming, and costly task. Hence, this study aims to develop a comprehensive design model using ANN along with the Adam optimization function to predict the compressive strength of fly ash-based geopolymer concrete. The significance of the proposed model in this study lies in considering a wide range of design parameters (10 input variables), leading to improved results. In other words, quantitative studies have been conducted on the impact of other essential input features, such as NaOH concentration, curing conditions, and mix ratio, on GPC compressive strength, opening up a potential range of advancements for future research endeavors.

2- Methodology

2-1- Data set

The data for this study were gathered from published papers spanning the years 2000 to 2020. This dataset comprises 162 samples of fly ash-based geopolymer concrete tested in the laboratory with various mix designs (as input features) and compressive strength (as the output parameter). The dataset, along with their references, is presented in Table 1. Considering the chemical composition of fly ash, the constituent material ratio, and the curing time and temperature, ten parameters were selected as inputs for the model. These parameters include the ratio of water to total solid materials of fly ash and the solution of sodium hydroxide and sodium silicate, the ratio of total solution of sodium hydroxide and sodium silicate to the amount of fly ash, the ratio of sodium silicate to sodium hydroxide, the chemical composition index (CCI) of fly ash, the total aggregate content relative to the total weight of geopolymer concrete, the coarse aggregate content relative to the total aggregate content, the curing duration, curing temperature, the ratio of plasticizer to fly ash content, and the molarity of sodium hydroxide. The expression of CCI is shown in Eq. (1) (Khalaf et al. 2022). Additionally, the model's output parameter (target) is the compressive strength of fly ash-based GPC. It's important to highlight that all the inputs under consideration are mutually independent. It should be noted, the input data considered in this study include the most influential input features from several recently published articles. Figure 1 illustrates the procedure of conducting this analysis.

$$CCI = \frac{Na_2O + CaO}{SiO_2 + Al_2O_3 + Fe_2O_3} \quad (1)$$

Data normalization is a fundamental step in various soft computing techniques and is crucial for achieving optimal performance in machine learning algorithms. Inadequately scaled input and output variables can significantly hinder the training process, leading to slow convergence or instability. Consequently, scaling variables appropriately can enhance the training process's accuracy and speed (García et al., 2015). Linear normalization, a commonly employed scaling method, is designed to rescale all numerical values of input or output attributes from 0 to 1. This normalization technique can be achieved using the following equation (2):

$$y = \frac{x - \min(x)}{\max(x) - \min(x)} \quad (2)$$

where x, y, $min(x)$, and $max(x)$ represent the original, normalized, minimum, and maximum values of the respective variable.

The correlation coefficient table (Table 2) presents the pairwise correlation coefficients among the variables under study. These coefficients provide insights into the strength and direction of the relationships between different variables.

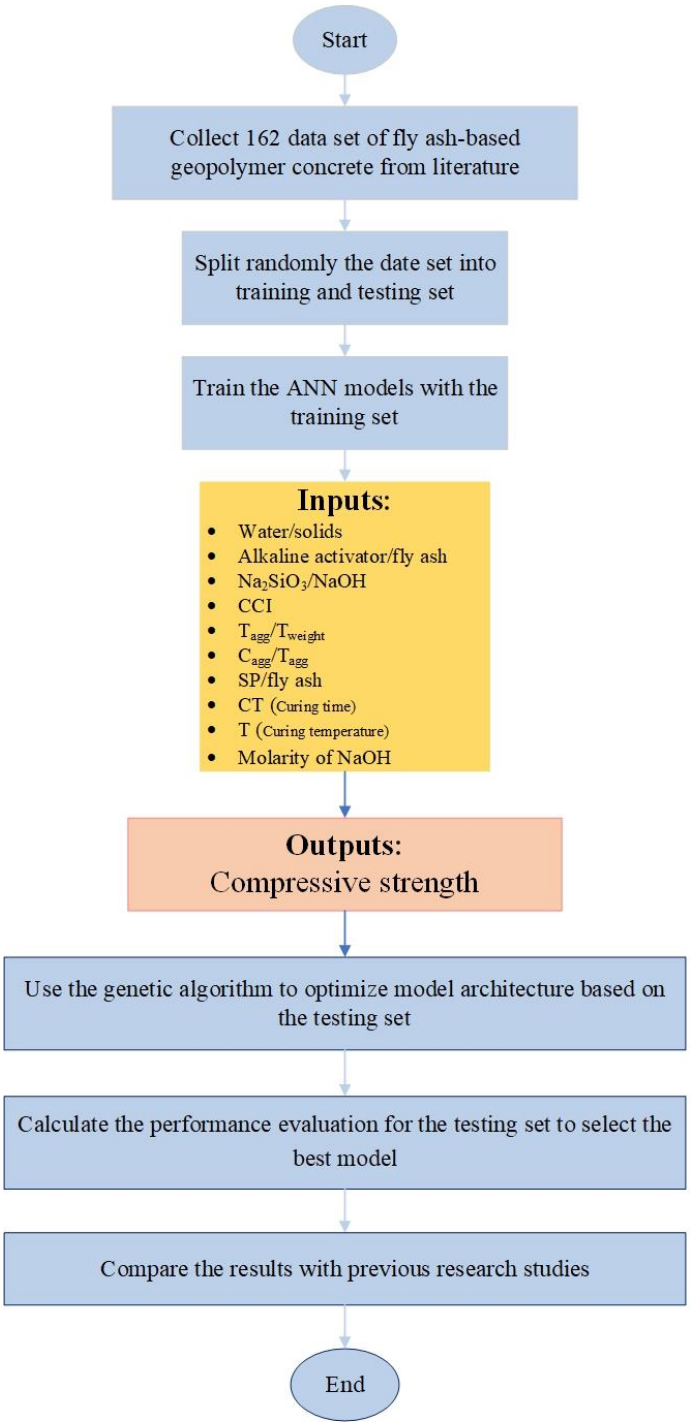

Figure. 1. Depiction of the steps involved in conducting experiments.

Table 1. Statistical characteristics of the data set.

Parameter	Explanation Parameter	Unit	Abb[1]	Variable Type	Min	Max	AVG[2]	SD[3]	Median	VAR[4]	SEM[5]
Water/solids	The ratio of the amount of water to the total solids of fly ash and sodium hydroxide solution and sodium silicate solution	w/w	W/S	Input	0.253	0.408	0.174	0.044	0.250	0.0019	0.0034
Alkaline activator/fly ash	The total ratio of sodium hydroxide and sodium silicate solution to the amount of fly ash	w/w	AA/FA	Input	0.300	0.814	0.457	0.100	0.449	0.0102	0.0079
Na_2SiO_3/NaOH	The ratio of sodium silicate to sodium hydroxide	w/w	SS/SH	Input	0.400	4.000	2.388	0.462	2.5	0.2149	0.0364
CCI	Chemical composition index of fly ash	%	CCI	Input	0.633	9.402	2.630	1.884	2.310	3.5697	0.1484
T_{agg}/T_{weight}	The total amount of aggregate relative to the total weight of geopolymer concrete	w/w	T_a/T_w	Input	0.680	0.832	0.763	0.032	0.763	0.0010	0.0025
C_{agg}/T_{agg}	The amount of coarse grain to the total amount of aggregate	w/w	C_a/T_a	Input	0.416	0.805	0.652	0.058	0.650	0.0032	0.0048
SP/fly ash	The ratio of the amount of superplasticizer to the amount of fly ash	w/w	SP/FA	Input	0.000	0.070	0.019	0.015	0.019	0.0002	0.0012
CT	Curing time	hour	CT	Input	24.000	96.000	26.370	8.928	24	80.210	0.7036
T	Curing temperature	^0C	T	Input	60.000	100.00	26.370	15.992	80	257.34	1.2603
Molarity of NaOH	Molarity of sodium hydroxide	mol/L	M_{SH}	Input	8.000	16.000	11.451	2.085	10	4.373	0.1643
Compressive strength	Compressive strength	MPa	CS	Output	17.000	74.00	43.130	10.540	42	111.77	0.8306

1.Abbreviation; 2. Average; 3. Standard Deviation; 4. Variance; 5. Standard Error of the Mean.

Table 2. Correlation coefficient of the data set.

	W/S	AA/FA	SS/SH	CCI	T_a/T_w	C_a/T_a	SP/FA	CT	T	M_{SH}	CS
W/S	1										
AA/FA	0.4847	1									
SS/SH	0.0399	0.1638	1								
CCI	0.4789	0.1179	0.158	1							
T_a/T_w	-0.1283	0.1775	0.2303	-0.1996	1						
C_a/T_a	-0.4251	-0.035	-0.121	-0.5528	0.1981	1					
SP/FA	0.5949	0.1881	0.1644	0.7616	-0.085	-0.4231	1				
CT	0.3099	-0.004	0.0646	0.4254	-0.279	-0.3318	0.5371	1			
T	0.1523	0.4088	0.3015	-0.1372	0.4377	0.132	-0.0147	-0.16	1		
M_{SH}	-0.1689	-0.394	-0.249	-0.0663	-0.455	0.0212	-0.0063	0.181	-0.5089	1	
CS	-0.4555	-0.089	0.1949	0.1436	0.0037	0.0387	-0.0346	-0.01	0.0058	0.0873	1

2-2- ANN modelling

ANNs are computational models that aim to emulate the human brain and its functions using a set of interconnected elements. They can address problems such as identification, control, optimization, and solving differential equations. The overall architecture of artificial neural networks is fine-tuned and optimized through a learning or training algorithm until it achieves the desired functionality. An ANN model comprises numerous complex and nonlinear artificial neurons interconnected by weights, as illustrated in Figure 2. These weights determine the influence of input features from the preceding layer on the learning process and can be adjusted to generate the desired output.

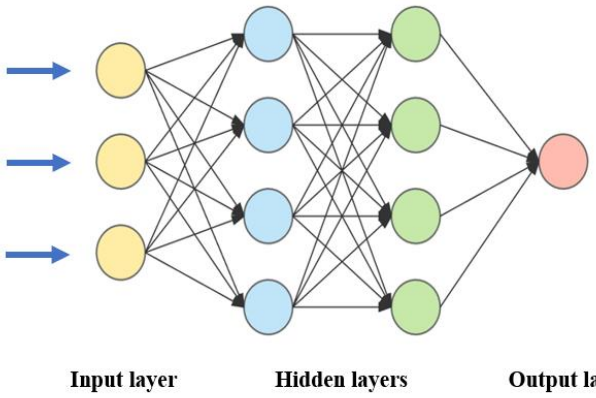

Figure.2. Schematic of ANN

The ANN model transmits information from the input layer to the output layer. During the learning process, the network minimizes the disparity between actual and predicted values. In many instances, ANN acts as an adaptive system, capable of altering its model based on the relevant information flowing through the network during the learning phase. ANN has the capability to learn and decipher highly intricate relationships between input and output data (Malekian and Chitsaz, 2021).

2-3- Model setup

This study randomly divided the dataset into two sets: a training dataset for model learning and a testing dataset for model evaluation. It is worth mentioning that 80 and 20 percent of data were used for training and testing the models, respectively.

Table 3. Selected data and their references.

Chemical composition of fly ash (percent)					Fly Ash (Kg/m)	C_{agg} (Kg/m³)	F_{agg} (Kg/m³)	NaOH (SH) (Kg/m³)	sodium hydroxide (SS) (Kg/m³)	Extra water (Kg/m³)	SP (Kg/m³)	Molarity Of SH	Percentage of SiO_2 in SS	Percentage of NA_2O in SS	curing time (h)	Curing temp (C)	Compressive strength (Mpa)	Ref
SiO2	Na2O	CaO	Al2O3	Fe2O3														
51.19	2.12	5.57	24	6.6	400	950	850	57	143	40	28	12	29.43	14.26	24	70	53.46	(Ahmed et al., 2011)
51.19	2.12	5.57	24	6.6	400	950	850	57	143	48	28	12	29.43	14.26	24	70	45.01	
51.19	2.12	5.57	24	6.6	400	950	850	57	143	60	28	12	29.43	14.26	24	70	37.31	
51.19	2.12	5.57	24	6.6	400	950	850	57	143	80	28	12	29.43	14.26	24	70	22.58	
51.19	2.12	5.57	24	6.6	400	950	850	57	143	48	28	12	29.43	14.26	48	70	51.03	
51.19	2.12	5.57	24	6.6	400	950	850	57	143	48	28	12	29.43	14.26	72	70	51.41	
51.19	2.12	5.57	24	6.6	400	950	850	57	143	48	28	12	29.43	14.26	96	70	51.68	
51.19	2.12	5.57	24	6.6	400	950	850	57	143	48	28	12	29.43	14.26	48	60	44.81	
51.19	2.12	5.57	24	6.6	400	950	850	57	143	48	28	12	29.43	14.26	48	80	48.56	
51.19	2.12	5.57	24	6.6	400	950	850	57	143	48	28	12	29.43	14.26	48	90	47.99	
53.36	0.37	1.34	26.49	10.86	476	1294	554	120	48	0	0	8	29.4	14.7	24	60	17	(Hardjito and Rangan, 2005)
53.36	0.37	1.34	26.49	10.86	476	1294	554	48	120	0	0	8	29.4	14.7	24	60	57	
53.36	0.37	1.34	26.49	10.86	476	1294	554	48	120	0	0	8	29.4	14.7	24	90	66	
53.36	0.37	1.34	26.49	10.86	476	1294	554	120	48	0	0	14	29.4	14.7	24	60	48	
53.36	0.37	1.34	26.49	10.86	476	1294	554	48	120	0	0	14	29.4	14.7	24	60	68	
53.36	0.37	1.34	26.49	10.86	476	1294	554	48	120	0	0	14	29.4	14.7	24	90	70	
47.8	0.31	2.42	24.4	17.4	408	1201	647	41	103	0	6.1	8	29.4	14.7	24	60	63	(Hardjito et al., 2005)
53.36	0.37	1.34	26.49	10.86	408	1294	554	41	103	0	8.2	14	29.4	14.7	24	60	59	
53.36	0.37	1.34	26.49	10.86	408	1294	554	41	103	0	8.2	14	29.4	14.7	24	75	65	
53.36	0.37	1.34	26.49	10.86	408	1294	554	41	103	0	8.2	14	29.4	14.7	24	90	71	
53.36	0.37	1.34	26.49	10.86	408	1294	554	41	103	10.7	8.2	14	29.4	14.7	24	75	60	
53.36	0.37	1.34	26.49	10.86	408	1294	554	41	103	10.7	8.2	14	29.4	14.7	24	90	59	
53.36	0.37	1.34	26.49	10.86	408	1294	554	41	103	21.3	8.2	14	29.4	14.7	24	60	44	
53.36	0.37	1.34	26.49	10.86	408	1294	554	41	103	21.3	8.2	14	29.4	14.7	24	75	44	
53.36	0.37	1.34	26.49	10.86	408	1294	554	41	103	21.3	8.2	14	29.4	14.7	24	90	44	
47.8	0.31	2.42	24.4	17.4	408	1201	647	41	103	0	6.1	8	29.4	14.7	24	60	55	
47.8	0.31	2.42	24.4	17.4	408	1201	647	41	103	7.5	6.1	10	29.4	14.7	24	60	53	
47.8	0.31	2.42	24.4	17.4	408	1201	647	41	103	14.4	6.1	12	29.4	14.7	24	60	51	
47.8	0.31	2.42	24.4	17.4	408	1201	647	41	103	20.7	6.1	14	29.4	14.7	24	60	45	
47.8	0.31	2.42	24.4	17.4	408	1201	647	41	103	26.5	6.1	16	29.4	14.7	24	60	47	
47.8	0.31	2.42	24.4	17.4	408	1201	647	41	103	0	6.1	8	29.4	14.7	24	90	68	
47.8	0.31	2.42	24.4	17.4	408	1201	647	55.4	103	0	6.1	8	29.4	14.7	24	60	55	

Table3. Continued

Chemical composition of fly ash (percent)					Fly Ash (Kg/m)	C_{agg} (Kg/m^3)	F_{agg} (Kg/m^3)	NaOH (SH) (Kg/m^3)	Sodium hydroxide (SS) (Kg/m^3)	Extra water (Kg/m^3)	SP (Kg/m^3)	Molarity Of SH	Percentage of SiO_2 in SS	Percentage of Na_2O in SS	curing time (h)	Curing temp (C)	Compressive strength (Mpa)	Ref
SiO2	Na_2O	CaO	Al_2O_3	Fe_2O_3														
50.5	0.45	2.13	26.6	13.8	394	1201	647	52.57	105.14	21.47	6.1	14	29.4	14.7	24	60	29.71	(Olivia and Nikraz, 2012)
50.5	0.45	2.13	26.6	13.8	409	1177	623	57.24	85.87	24.46	6.1	14	29.4	14.7	24	75	35.73	
50.5	0.45	2.13	26.6	13.8	444	1177	623	44.44	111.11	18.55	6.1	14	29.4	14.7	24	60	38.69	
50.5	0.45	2.13	26.6	13.8	498	1153	599	59.82	89.72	26.47	6.1	14	29.4	14.7	24	60	39.93	
50.5	0.45	2.13	26.6	13.8	462	1177	623	46.15	92.31	18.61	6.1	14	29.4	14.7	24	75	42.51	
50.5	0.45	2.13	26.6	13.8	463	1153	599	52.9	132.24	21.23	6.1	14	29.4	14.7	24	75	49.6	
50.5	0.45	2.13	26.6	13.8	408	1201	647	62	93	4	0	14	28.9	14.7	24	60	32	(Sarker et al., 2013)
50.5	0.45	2.13	26.6	13.8	408	1201	647	62	93	0	0	14	28.9	14.7	24	60	36	
50.5	0.45	2.13	26.6	13.8	408	1201	647	68	103	0	0	14	28.9	14.7	24	60	48	
65.4	0	1.26	20.7	6.2	378	1294	554	50	124	0	8	12	29.4	14.7	24	70	35.48	(Sujata et al., 2012)
65.4	0	1.26	20.7	6.2	408	1201	647	63	138	0	8	12	29.4	14.7	24	70	53.5	
57.3	0.73	0.03	27.13	8.06	428	1170	630	57	114	43	4.3	10	35.01	16.84	24	75	35	(Vora and Dave, 2013)
57.3	0.73	0.03	27.13	8.06	428	1170	630	57	114	43	4.3	12	35.01	16.84	24	75	43	
57.3	0.73	0.03	27.13	8.06	428	1170	630	57	114	43	4.3	14	35.01	16.84	24	75	46	
57.3	0.73	0.03	27.13	8.06	428	1170	630	57	114	43	4.3	14	35.01	16.84	24	60	38	
57.3	0.73	0.03	27.13	8.06	428	1170	630	57	114	43	4.3	14	35.01	16.84	24	75	46	
57.3	0.73	0.03	27.13	8.06	428	1170	630	57	114	43	4.3	14	35.01	16.84	24	90	49	
57.3	0.73	0.03	27.1	8.1	428	1170	630	49	122	43	8.5	14	35.01	16.84	24	75	30	
57.3	0.73	0.03	27.1	8.1	444	1170	630	44	111	43	9	14	35.01	16.84	24	75	30	
57.3	0.73	0.03	27.1	8.1	428	1170	630	57	114	43	8.5	14	35.01	16.84	24	75	40	
57.3	0.73	0.03	27.13	8.1	428	1170	630	49	122	43	8.5	14	35.01	16.84	24	75	28	
57.3	0.73	0.03	27.13	8.06	428	1170	630	49	122	43	8.5	14	35.01	16.84	48	75	32	
57.3	0.73	0.03	27.13	8.06	428	1170	630	49	122	43	8.5	14	35.01	16.84	48	75	30	
57.3	0.73	0.03	27.13	8.06	428	1170	630	49	122	43	8.5	14	35.01	16.84	48	75	32	
57.3	0.73	0.03	27.13	8.06	428	1170	630	49	122	43	13	14	35.01	16.84	48	75	30	
57.3	0.73	0.03	27.13	8.06	428	1170	630	49	122	43	17	14	35.01	16.84	48	75	29	
57.3	0.73	0.03	27.13	8.06	428	1170	630	49	122	43	8.5	14	35.01	16.84	48	75	36	
57.3	0.73	0.03	27.13	8.06	428	1170	630	49	122	43	8.5	14	35.01	16.84	48	75	45	
57.3	0.73	0.03	27.13	8.06	428	1170	630	57	114	43	4.3	14	35.01	16.84	24	75	30	
57.3	0.73	0.03	27.13	8.06	428	1170	630	57	114	64	4.3	14	35.01	16.84	24	75	24	
57.3	0.73	0.03	27.13	8.06	428	1170	630	57	114	86	4.3	14	35.01	16.84	24	75	20	
57.3	0.73	0.03	27.13	8.06	428	1170	630	57	114	43	4.3	8	35.01	16.84	24	75	32	

Table 3. Continued

Chemical composition of fly ash (percent)					Fly Ash (Kg/m)	C_{agg} (Kg/m^3)	F_{agg} (Kg/m^3)	NaOH (SH) (Kg/m^3)	Sodium hydroxide (SS) (Kg/m^3)	Extra water (Kg/m^3)	SP (Kg/m^3)	Molarity Of SH	Percentage of SiO_2 in SS	Percentage of Na_2O in SS	curing time (h)	Curing temp (C)	Compressive strength (Mpa)	Ref
SiO_2	Na_2O	CaO	Al_2O_3	Fe_2O_3														
47.9	0.4	3.8	28	14.1	410	1044.4	530.6	67.1	117.4	79.2	0	10	29.4	14.7	24	80	28.3	(Lokuge et al., 2018)
47.9	0.4	3.8	28	14.1	410	1157.5	588	51.2	153.8	0.75	0	10	29.4	14.7	24	80	42.1	
47.9	0.4	3.8	28	14.1	410	1162	590.2	41	143.5	11.9	0	10	29.4	14.7	24	80	49	
47.9	0.4	3.8	28	14.1	410	1154.9	586.8	41	164	2.6	0	10	29.4	14.7	24	80	55.5	
61.89	0.4	0.87	28.05	4.11	500	1321	320	80	120	0	6	16	23	11.5	24	60	53.56	(Pavithra et al., 2016)
61.89	0.4	0.87	28.05	4.11	400	1419	344	80	120	0	4	16	23	11.5	24	60	45.95	
61.89	0.4	0.87	28.05	4.11	330	1165	360	80	120	0	3.2	16	23	11.5	24	60	37.12	
62.2	0.52	2.27	27.5	3.92	410	1164	627	61.5	123	45	22.5	12	29.4	14.7	24	80	35.91	(Fatima et al., 2019)
62.2	0.52	2.27	27.5	3.92	480	1140	606	56	112	35	12.5	14	29.4	14.7	24	80	65.11	
53.8	1.25	0.9	21.2	17	420	1124	688	48	120	0	0	8	29.4	14.7	24	100	37	(Gopalakrishnan, 2018)
53.8	1.25	0.9	21.2	17	420	1124	688	48	120	0	0	10	29.4	14.7	24	100	43	
53.8	1.25	0.9	21.2	17	420	1124	688	48	120	0	0	12	29.4	14.7	24	100	50	
53.8	1.25	0.9	21.2	17	420	1124	688	48	120	0	0	14	29.4	14.7	24	100	55	
53.8	1.25	0.9	21.2	17	420	1124	688	48	120	0	0	16	29.4	14.7	24	100	67	
51.75	1.35	1.4	34.75	6	500	78	1100	65	163	25	0	12	29.8	14.7	24	60	40.2	(Patel and Shah, 2018)
51.75	1.35	1.4	34.75	6	500	785	1100	65	163	25	0	12	29.8	14.7	24	70	42.7	
48	0.39	1.76	29	12.7	404	1190	640	41	102	25.5	6	14	29.4	14.7	24	60	39.5	(Sumajouw and Rangan, 2006)
48	0.39	1.76	29	12.7	404	1190	640	41	102	17	6	14	29.4	14.7	24	60	49.5	
48	0.39	1.76	29	12.7	404	1190	640	41	103	13.5	6	14	29.4	14.7	24	60	74	
47.8	0.31	2.42	24.4	17.4	408	1202	647	41	103	26	6	16	29.4	14.7	24	60	41.5	
47.8	0.31	2.42	24.4	17.4	408	1202	647	41	102	16.5	6	14	29.4	14.7	24	60	62.5	
70.3	0.4	0.2	23.1	1.4	409	909	686	129	204	10	0	11	29.4	14.7	24	80	22.4	(Joseph and Mathew, 2012)
59.7	0.04	2.1	28.36	4.57	421	1273	318	66	165	5	8	10	34.64	16.27	24	100	38	
59.7	0.04	2.1	28.36	4.57	421	1196	395	66	165	5	8	10	34.64	16.27	24	100	39	
59.7	0.04	2.1	28.36	4.57	421	1112	477	66	165	5	8	10	34.64	16.27	24	100	40	
59.7	0.04	2.1	28.36	4.57	421	1032	556	66	165	5	8	10	34.64	16.27	24	100	45	
59.7	0.04	2.1	28.36	4.57	421	949	633	66	165	5	8	10	34.64	16.27	24	100	39	

Table 3. Continued

Chemical composition of fly ash (percent)					Fly Ash (Kg/m)	C_{ssz} (Kg/m^3)	F_{ssz} (Kg/m^3)	NaOH (SH) (Kg/m^3)	Sodium hydroxide (SS) (Kg/m^3)	Extra water (Kg/m^3)	SP (Kg/m^3)	Molarity Of SH	Percentage of SiO_2 in SS	Percentage of Na_2O in SS	curing time (h)	Curing temp (C)	Compressive strength (Mpa)	Ref
SiO_2	Na_2O	CaO	Al_2O_3	Fe_2O_3														
59.7	0.04	2.1	28.36	4.57	365	1379	335	60	151	0	7	10	34.64	16.27	24	100	40	(Joseph and Mathew, 2012)
59.7	0.04	2.1	28.36	4.57	365	1295	427	60	151	0	7	10	34.64	16.27	24	100	41	
59.7	0.04	2.1	28.36	4.57	365	1205	516	60	151	0	7	10	34.64	16.27	24	100	42	
59.7	0.04	2.1	28.36	4.57	365	1118	602	60	151	0	7	10	34.64	16.27	24	100	47	
59.7	0.04	2.1	28.36	4.57	365	1028	685	60	151	0	7	10	34.64	16.27	24	100	42	
59.7	0.04	2.1	28.36	4.57	310	1485	371	49	122	4	6	10	34.64	16.27	24	100	42	
59.7	0.04	2.1	28.36	4.57	310	1395	460	49	122	4	6	10	34.64	16.27	24	100	44	
59.7	0.04	2.1	28.36	4.57	310	1298	556	49	122	4	6	10	34.64	16.27	24	100	45	
59.7	0.04	2.1	28.36	4.57	310	1204	648	49	122	4	6	10	34.64	16.27	24	100	56	
59.7	0.04	2.1	28.36	4.57	310	1107	738	49	122	4	6	10	34.64	16.27	24	100	46	
59.7	0.04	2.1	28.36	4.57	255	1591	398	40	100	3	5	10	34.64	16.27	24	100	33	
59.7	0.04	2.1	28.36	4.57	255	1495	493	40	100	3	5	10	34.64	16.27	24	100	35	
59.7	0.04	2.1	28.36	4.57	255	1390	596	40	100	3	5	10	34.64	16.27	24	100	40	
59.7	0.04	2.1	28.36	4.57	255	1290	695	40	100	3	5	10	34.64	16.27	24	100	49	
59.7	0.04	2.1	28.36	4.57	255	1155	791	40	100	3	5	10	34.64	16.27	24	100	41	
59.7	0.04	2.1	28.36	4.57	330	1204	648	46	69	29	7	10	34.64	16.27	24	100	31	
59.7	0.04	2.1	28.36	4.57	327	1204	648	38	76	31	7	10	34.64	16.27	24	100	34	
59.7	0.04	2.1	28.36	4.57	326	1204	648	33	81	32	7	10	34.64	16.27	24	100	39	
59.7	0.04	2.1	28.36	4.57	325	1204	648	28	85	33	6	10	34.64	16.27	24	100	36	
59.7	0.04	2.1	28.36	4.57	324	1204	648	25	88	34	6	10	34.64	16.27	24	100	34	
59.7	0.04	2.1	28.36	4.57	322	1204	648	58	87	14	6	10	34.64	16.27	24	100	34	
59.7	0.04	2.1	28.36	4.57	319	1204	648	48	96	16	6	10	34.64	16.27	24	100	40	
59.7	0.04	2.1	28.36	4.57	318	1204	648	41	102	17	6	10	34.64	16.27	24	100	47	
59.7	0.04	2.1	28.36	4.57	316	1204	648	36	107	19	6	10	34.64	16.27	24	100	43	
59.7	0.04	2.1	28.36	4.57	315	1204	648	32	110	20	6	10	34.64	16.27	24	100	38	
59.7	0.04	2.1	28.36	4.57	314	1204	648	69	104	0	6	10	34.64	16.27	24	100	47	
59.7	0.04	2.1	28.36	4.57	312	1204	648	57	114	2	6	10	34.64	16.27	24	100	53	
59.7	0.04	2.1	28.36	4.57	310	1204	648	49	122	4	6	10	34.64	16.27	24	100	58	
59.7	0.04	2.1	28.36	4.57	308	1204	648	42	127	5	6	10	34.64	16.27	24	100	52	
59.7	0.04	2.1	28.36	4.57	307	1204	648	38	131	6	6	10	34.64	16.27	24	100	42	
59.7	0.04	2.1	28.36	4.57	293	1204	648	76	114	0	6	10	34.64	16.27	24	100	41	
59.7	0.04	2.1	28.36	4.57	293	1204	648	63	127	0	6	10	34.64	16.27	24	100	42	
59.7	0.04	2.1	28.36	4.57	293	1204	648	54	136	0	6	10	34.64	16.27	24	100	43	
59.7	0.04	2.1	28.36	4.57	293	1204	648	48	143	0	6	10	34.64	16.27	24	100	42	
59.7	0.04	2.1	28.36	4.57	293	1204	648	42	148	0	6	10	34.64	16.27	24	100	41	
59.7	0.04	2.1	28.36	4.57	330	1204	648	33	83	29	7	10	34.64	16.27	24	100	40	

Table 3. Continued

Chemical composition of fly ash (percent)					Fly Ash (Kg/m)	C_{agg} (Kg/m^3)	F_{agg} (Kg/m^3)	NaOH (SH) (Kg/m^3)	Sodium hydroxide (SS) (Kg/m^3)	Extra water (Kg/m^3)	SP (Kg/m^3)	Molarity Of SH	Percentage of SiO_2 in SS	Percentage of NA_2O in SS	curing time (h)	Curing temp (C)	Compressive strength (Mpa)	Ref
SiO_2	Na_2O	CaO	Al_2O_3	Fe_2O_3														
59.7	0.04	2.1	28.36	4.57	321	1204	648	32	80	35	6	10	34.64	16.27	24	100	38	(Joseph and Mathew, 2012)
59.7	0.04	2.1	28.36	4.57	314	1204	648	31	78	42	6	10	34.64	16.27	24	100	35	
59.7	0.04	2.1	28.36	4.57	304	1204	648	30	76	48	6	10	34.64	16.27	24	100	31	
59.7	0.04	2.1	28.36	4.57	298	1204	648	30	74	53	6	10	34.64	16.27	24	100	30	
59.7	0.04	2.1	28.36	4.57	332	1204	648	41	104	16	6	10	34.64	16.27	24	100	48	
59.7	0.04	2.1	28.36	4.57	314	1204	648	40	101	21	6	10	34.64	16.27	24	100	45	
59.7	0.04	2.1	28.36	4.57	305	1204	648	39	98	28	6	10	34.64	16.27	24	100	41	
59.7	0.04	2.1	28.36	4.57	297	1204	648	38	95	34	6	10	34.64	16.27	24	100	38	
59.7	0.04	2.1	28.36	4.57	290	1204	648	37	93	40	6	10	34.64	16.27	24	100	35	
59.7	0.04	2.1	28.36	4.57	314	1204	648	49	123	0	5	10	34.64	16.27	24	100	59	
59.7	0.04	2.1	28.36	4.57	306	1204	648	48	120	7	6	10	34.64	16.27	24	100	56	
59.7	0.04	2.1	28.36	4.57	298	1204	648	47	117	15	6	10	34.64	16.27	24	100	52	
59.7	0.04	2.1	28.36	4.57	290	1204	648	46	114	21	6	10	34.64	16.27	24	100	48	
59.7	0.04	2.1	28.36	4.57	282	1204	648	44	111	28	6	10	34.64	16.27	24	100	46	
59.7	0.04	2.1	28.36	4.57	293	1204	648	41	136	0	6	10	34.64	16.27	24	100	48	
59.7	0.04	2.1	28.36	4.57	293	1204	648	49	136	0	6	10	34.64	16.27	24	100	45	
59.7	0.04	2.1	28.36	4.57	290	1204	648	54	135	2	6	10	34.64	16.27	24	100	42	
59.7	0.04	2.1	28.36	4.57	282	1204	648	52	131	9	6	10	34.64	16.27	24	100	38	
59.7	0.04	2.1	28.36	4.57	275	1204	648	51	128	16	6	10	34.64	16.27	24	100	35	
59.7	0.04	2.1	28.36	4.57	326	1204	648	33	81	32	7	10	34.64	16.27	24	60	28	
59.7	0.04	2.1	28.36	4.57	318	1204	648	41	102	17	6	10	34.64	16.27	24	60	32	
59.7	0.04	2.1	28.36	4.57	310	1204	648	49	122	4	6	10	34.64	16.27	24	60	37	
59.7	0.04	2.1	28.36	4.57	293	1204	648	54	136	0	6	10	34.64	16.27	24	60	34	
59.7	0.04	2.1	28.36	4.57	326	1204	648	33	81	32	7	10	34.64	16.27	24	70	30	
59.7	0.04	2.1	28.36	4.57	318	1204	648	41	102	17	6	10	34.64	16.27	24	70	34	
59.7	0.04	2.1	28.36	4.57	310	1204	648	49	122	4	6	10	34.64	16.27	24	70	41	
59.7	0.04	2.1	28.36	4.57	293	1204	648	54	136	0	6	10	34.64	16.27	24	70	38	
59.7	0.04	2.1	28.36	4.57	326	1204	648	33	81	32	7	10	34.64	16.27	24	80	31	
59.7	0.04	2.1	28.36	4.57	318	1204	648	41	102	17	6	10	34.64	16.27	24	80	35	
59.7	0.04	2.1	28.36	4.57	310	1204	648	49	122	4	6	10	34.64	16.27	24	80	44	
59.7	0.04	2.1	28.36	4.57	326	1204	648	33	81	32	7	10	34.64	16.27	24	90	37	
59.7	0.04	2.1	28.36	4.57	318	1204	648	41	102	17	6	10	34.64	16.27	24	90	38	
59.7	0.04	2.1	28.36	4.57	310	1204	648	49	122	4	6	10	34.64	16.27	24	90	49	
59.7	0.04	2.1	28.36	4.57	293	1204	648	54	136	0	6	10	34.64	16.27	24	90	42	

ANN generally comprises an input layer, one or more hidden layers, neurons, an activation function, weights, a bias, and an output layer. Most network calculations and processing occur within the hidden layers situated between the input and output layers. The parameters of this network were optimized using the Adam optimization method. The architecture of this model included a maximum of two hidden layers, each hidden layer containing a maximum of 25 neurons. The Adam optimizer was selected as the optimization algorithm for ANN due to its ease of implementation, efficient computation, and minimal memory requirements (Kingma and Ba, 2014). Additionally, the ReLU function served as the activation function in the model.

2-4- Performance evaluation

The accuracy indices in equations (3-6) have been provided. These indices were selected to compare the results with previous studies and assess the model's accuracy under study. The coefficient of determination (R^2) in equation (3) ranges between 0 and 1. This value indicates the linear correlation between the predicted and actual values (provided by the articles). When this coefficient is closer to one, the model performs better. The root mean square error (RMSE) indicates the value of the root mean square of the residual errors, as presented in equation (4). The mean absolute percentage error (MAPE) is the average of the absolute percentage errors obtained using equation (5). The mean absolute error (MAE) represents the absolute value of the difference between the predicted value and the actual value, calculated as shown in equation (6). Generally, the lower value of RMSE, MAPE, and MAE implies the higher accuracy of a regression model.

$$R^2 = 1 - \frac{\sum_{i=1}^{N}(y_i - \hat{y}_i)^2}{\sum_{i=1}^{N}(y_i - y_{avg})^2} \quad (3)$$

$$RMSE = \sqrt{\frac{\sum_{i=1}^{N}(y_i - \hat{y}_i)^2}{N}} \quad (4)$$

$$MAPE = \frac{100}{N}\sum_{i=1}^{N}\left|\frac{y_i - \hat{y}_i}{\hat{y}_i}\right| \quad (5)$$

$$MAE = \frac{\sum_{i=1}^{N}|y_i - \hat{y}_i|}{N} \quad (6)$$

3- Results and Discussion

3-1- ANN Model

This section explains the prediction model for the compressive strength of geopolymer concrete based on fly ash using ANN. Table 3 presents the results of three models with the most negligible error for predicting compressive strength. The results are sorted based on the RMSE error for the test data. According to Table 3, the best ANN model proposed for this dataset has two hidden layers. Also, the number of neurons in the first and second hidden layers is 15 and 10, respectively. The RMSE value for this model is 3.56 MPa, which is significantly smaller compared to the average compressive strength of geopolymer concrete based on fly ash for the entire dataset, which is 43.130 MPa (presented in Table 1).

Table 4. Comparison of the top 3 ANN models based on the lowest RMSE error.

Case	N.O. of neurons in hidden layers	Split	index			
			R^2	RMSE (MPa)	MAPE (%)	MAE (MPa)
i	(15,10)	All	0.891	3.40	6.4	2.56
		Train	0.901	3.36	6.06	2.46
		Test	**0.828**	**3.56**	**7.74**	**2.91**
ii	(19,24)	All	0.916	2.98	4.53	1.85
		Train	0.939	2.61	3.55	1.52
		Test	0.770	4.11	8.37	3.18
iii	(20,8)	All	0.857	3.89	7.16	2.98
		Train	0.869	3.53	6.73	2.85
		Test	0.766	4.14	8.86	3.51

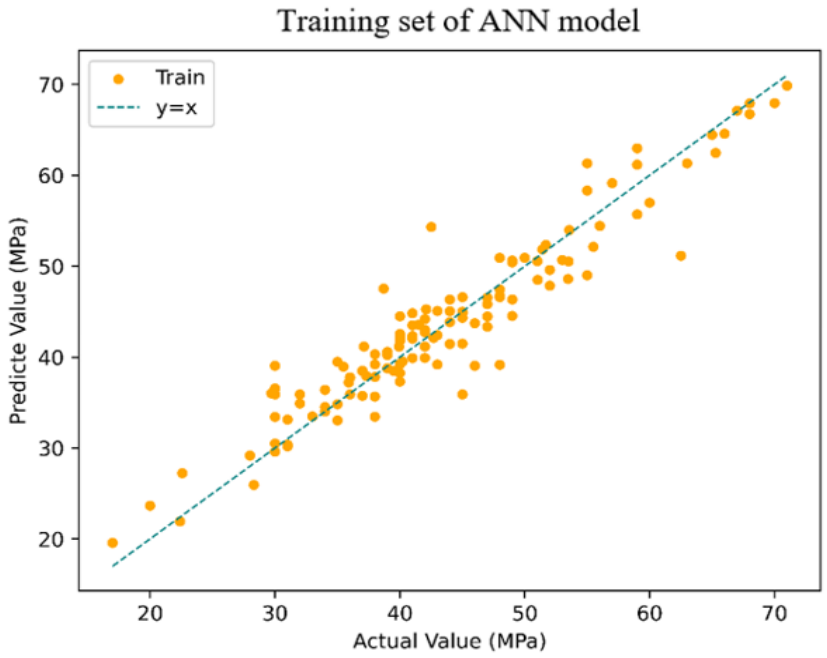

(a)

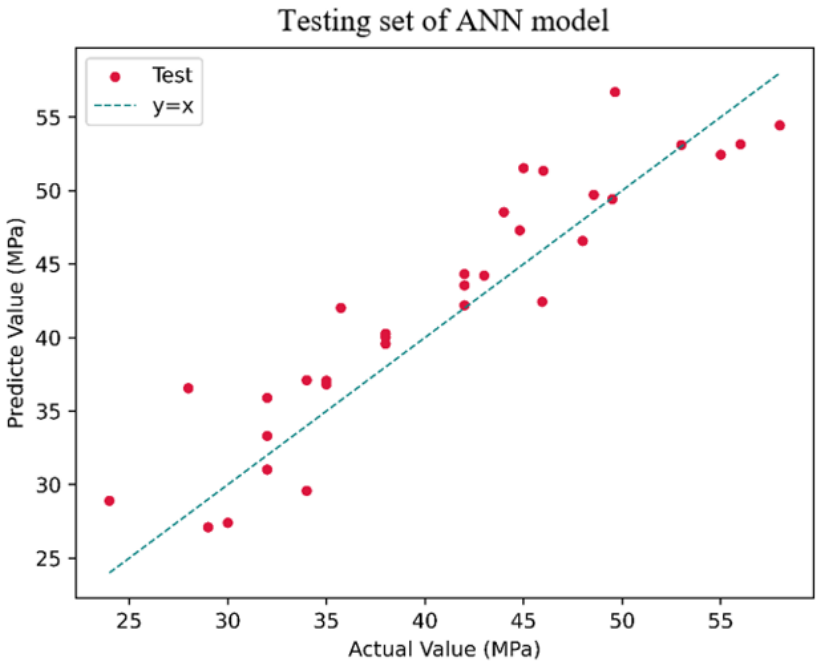

(b)

Figure. 3. Prediction results of fly ash-based geopolymer concrete compressive strength using ANN model, (a) for training data, (b) for test data.

In other words, it accounts for 8.25% of the input data average, which is very good. For this model, the MAPE value is 7.74%, indicating that the average absolute error percentage of the test data compared to the actual data is less than 8%, which is excellent. Additionally, the R^2 and MAE indices for the test data of this model are 0.828 and 2.91 MPa, respectively, all indicating the high accuracy of this model. The best model in Table 3 is highlighted in bold. Figure 3 shows the prediction

results of the compressive strength of geopolymer concrete based on fly ash using the ANN model. Figure 3 (a) and (b) are for training and test data, respectively. According to Figure 3, the proximity of prediction points around the blue dashed line indicates the high accuracy of this model.

3.2. Comparison of the present study with previous studies

This section compares the ANN model presented in this study with two recently published studies. Toufigh and Jafari (2021) utilized a Bayesian linear regression algorithm, while Lokuge et al. (2018) employed a multivariable adaptive regression splines (MARS) model to predict the compressive strength of geopolymer concrete based on fly ash. Toufigh and Jafari's model included 12 input features, and Lokuge et al. selected four input features in their MARS model. The summary of their study and current study are presented in Table 4. By comparing the present study with the studies mentioned above and evaluating the R^2, RMSE (MPa), MAPE (%), and MAE (MPa) indicators, it is evident that the present study exhibits significantly higher accuracy. It is worth mentioning that the samples examined in this study and Toufigh and Jafari's study are identical. Be aware that Table 4 is based on the indicators of the test data. For a better comparison of the results of Table 4, the RMSE parameter of all three studies is depicted in Figure 4.

Table 5. Comparison of the results of the present study with previous studies.

Case Study	NO. of input features	Sample size	Model	R^2	RMSE (MPa)	MAPE (%)	MAE (MPa)
Toufigh and Jafari (2021)	12	162	Bayesian linear regression	0.682	5.96	-	-
Lokuge et al. (2018)	4	96	MARS	-	16.37	-	10.96
Current study	10	162	MLP	0.828	3.56	7.74	2.91

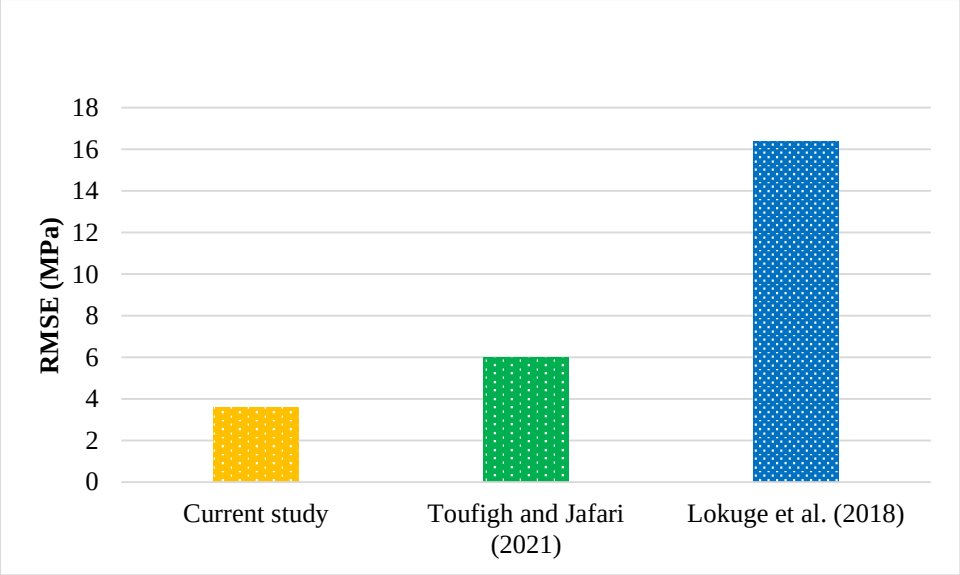

Figure.4. RMSE parameter of the present study with previous studies.

4- Conclusion

In this study, the compressive strength of geopolymer concrete based on fly ash was predicted using Python software with the aid of an artificial neural network (ANN). One hundred sixty-two datasets were collected from recent articles. The dataset was randomly divided into 80% training and 20% testing data. Ten input variables and one output

variable (compressive strength of geopolymer concrete based on fly ash) were investigated.

The best network of this model consisted of two hidden layers, with the number of neurons in the first and second layers being 15 and 10, respectively. The performance indices R^2, RMSE (MPa), MAPE (%), and MAE (MPa) were calculated as 0.828, 3.56 MPa, 7.74%, and 2.91 MPa, respectively, for the testing data. These values for the training data were 0.901, 3.36 MPa, 6.06%, and 2.46 MPa, respectively. Also, Comparing the ANN network with regression-based studies demonstrated superior performance by achieving better performance metrics for predicting compressive strength. In addition, based on the proposed optimal model and mix of design compositions used in this model, the design process can be facilitated cost-effectively in a shorter time while maintaining high flexibility for the designer.

This study proposes the development of an advanced web application to aid in understanding the model and optimizing mixing plans effectively. Additionally, it involves a comprehensive comparative analysis between machine learning and deep learning models, accompanied by the utilization of state-of-the-art optimizers. This analysis aims to enhance the efficiency and accuracy of predictive tasks related to mixing plan optimization, contributing to future advancements in the field.

Funding sources

There is no funding source.

Competing interest

Declaration of competing interest

The authors declare that they have no known competing financial interests or personal relationships that could have appeared to influence the work reported in this paper.

Authors contribution statement

E.M: *Conceptualization, Methodology, Software, Validation, Formal analysis, Investigation, Resources, Data curation, Writing – original draft, Visualization.* ***V.T.:*** *Methodology, Validation, Investigation, Resources, Writing – review & editing, Supervision.*

Reference

Ahmed, H. U., Mohammed, A. S., Mohammed, A. A., & Faraj, R. H. (2021). Systematic multiscale models to predict the compressive strength of fly ash-based geopolymer concrete at various mixture proportions and curing regimes. *Plos one*, *16*(6), e0253006.

Ahmed, M. F., Nuruddin, M. F., & Shafiq, N. (2011). Compressive strength and workability characteristics of low-calcium fly ash-based self-compacting geopolymer concrete. *International journal of civil and environmental engineering*, *5*(2), 64-70.

Al Bakri, A. M., Kamarudin, H., Bnhussain, M., Rafiza, A., & Zarina, Y. (2012). Effect of Na^ sub 2^ SiO^ sub 3^/NaOH Ratios and NaOH Molarities on Compressive Strength of Fly-Ash-Based Geopolymer. *ACI Materials Journal*, *109*(5), 503.

Almutairi, A. L., Tayeh, B. A., Adesina, A., Isleem, H. F., & Zeyad, A. M. (2021). Potential applications of geopolymer concrete in construction: A review. *Case Studies in Construction Materials*, *15*, e00733.

BKA, M. A. R., Ngamkhanong, C., Wu, Y., & Kaewunruen, S. (2021). Recycled aggregates concrete compressive strength prediction using artificial neural networks (ANNs). *Infrastructures*, *6*(2), 17.

Bu, L., Du, G., & Hou, Q. (2021). Prediction of the compressive strength of recycled aggregate concrete based on artificial neural network. *Materials*, *14*(14), 3921.

Davidovits, J. (1993). Geopolymer cements to minimize carbon dioxide greenhouse warming. *Ceram. Trans.*, *37*(1), 165-182.

Deshpande, N., Londhe, S., & Kulkarni, S. (2014). Modeling compressive strength of recycled aggregate concrete by Artificial Neural Network, Model Tree and Non-linear Regression. *International Journal of Sustainable Built Environment*, *3*(2), 187-198.

Fallah, S., & Nematzadeh, M. (2017). Mechanical properties and durability of high-strength concrete containing macro-polymeric and polypropylene fibers with nano-silica and silica fume. *Construction and Building Materials*, *132*, 170-187.

Farhan, N. A., Sheikh, M. N., & Hadi, M. N. (2019). Investigation of engineering properties of normal and high strength fly ash based geopolymer and alkali-activated slag concrete compared to ordinary Portland cement concrete. *Construction and Building Materials*, *196*, 26-42.

García, S., Luengo, J., & Herrera, F. (2015). *Data preprocessing in data mining* (Vol. 72). Springer.

Gholhaki, M., Hajforoush, M., & Kazemi, M. (2018). An investigation on the fresh and hardened properties of self-compacting concrete incorporating magnetic water with various pozzolanic materials. *Construction and Building Materials*, *158*, 173-180.

Gopalakrishnan, R. (2018). Influence of concentration of alkaline liquid on strength of GGBS and fly ash based alumina silicate CONCRETE. *Int. J. Civ. Eng. Technol*, *9*, 1229-1236.

Hansen, J., Johnson, D., Lacis, A., Lebedeff, S., Lee, P., Rind, D., & Russell, G. (1981). Climate impact of increasing atmospheric carbon dioxide. *Science*, *213*(4511), 957-966.

Hardjito, D., & Rangan, B. V. (2005). Development and properties of low-calcium fly ash-based geopolymer concrete.

Hardjito, D., Wallah, S. E., Sumajouw, D. M., & Rangan, B. V. (2005). Fly ash-based geopolymer concrete. *Australian Journal of Structural Engineering*, *6*(1), 77-86.

Hendriks, C. A., Worrell, E., De Jager, D., Blok, K., & Riemer, P. (1998). Emission reduction of greenhouse gases from the cement industry. Proceedings of the fourth international conference on greenhouse gas control technologies,

Jafari, A., & Toufigh, V. (2023). Developing a comprehensive prediction model for the compressive strength of slag-based alkali-activated concrete. *Journal of Sustainable Cement-Based Materials*, 1-18.

Joseph, B., & Mathew, G. (2012). Influence of aggregate content on the behavior of fly ash based geopolymer concrete. *Scientia Iranica*, *19*(5), 1188-1194.

Kamath, M. V., Prashanth, S., Kumar, M., & Tantri, A. (2024). Machine-learning-algorithm to predict the high-performance concrete compressive strength using multiple data. *Journal of Engineering, Design and Technology*, *22*(2), 532-560.

Khalaf, A. A., Kopecskó, K., & Merta, I. (2022). Prediction of the compressive strength of fly ash geopolymer concrete by an optimised neural

network model. *Polymers*, *14*(7), 1423.

Khambra, G., & Shukla, P. (2023). Novel machine learning applications on fly ash based concrete: an overview. *Materials Today: Proceedings*, *80*, 3411-3417.

Kingma, D. P., & Ba, J. (2014). Adam: A method for stochastic optimization. *arXiv preprint arXiv:1412.6980*.

Lokuge, W., Wilson, A., Gunasekara, C., Law, D. W., & Setunge, S. (2018). Design of fly ash geopolymer concrete mix proportions using Multivariate Adaptive Regression Spline model. *Construction and Building Materials*, *166*, 472-481.

Malekian, A., & Chitsaz, N. (2021). Concepts, procedures, and applications of artificial neural network models in streamflow forecasting. In *Advances in streamflow forecasting* (pp. 115-147). Elsevier.

McLellan, B. C., Williams, R. P., Lay, J., Van Riessen, A., & Corder, G. D. (2011). Costs and carbon emissions for geopolymer pastes in comparison to ordinary portland cement. *Journal of cleaner production*, *19*(9-10), 1080-1090.

Moein, M. M., Saradar, A., Rahmati, K., Mousavinejad, S. H. G., Bristow, J., Aramali, V., & Karakouzian, M. (2023). Predictive models for concrete properties using machine learning and deep learning approaches: A review. *Journal of Building Engineering*, *63*, 105444.

Olivia, M., & Nikraz, H. (2011). Strength and water penetrability of fly ash geopolymer conrete. *Journal of Engineering and Applied Sciences*, *6*(7), 70-78.

Olivia, M., & Nikraz, H. (2012). Properties of fly ash geopolymer concrete designed by Taguchi method. *Materials & Design (1980-2015)*, *36*, 191-198.

Patel, Y. J., & Shah, N. (2018). Development of self-compacting geopolymer concrete as a sustainable construction material. *Sustainable Environment Research*, *28*(6), 412-421.

Pavithra, P., Reddy, M. S., Dinakar, P., Rao, B. H., Satpathy, B., & Mohanty, A. (2016). A mix design procedure for geopolymer concrete with fly ash. *Journal of cleaner production*, *133*, 117-125.

Possan, E., Thomaz, W. A., Aleandri, G. A., Felix, E. F., & dos Santos, A. C. (2017). CO2 uptake potential due to concrete carbonation: A case study. *Case Studies in Construction Materials*, *6*, 147-161.

Sarker, P. K., Haque, R., & Ramgolam, K. V. (2013). Fracture behaviour of heat cured fly ash based geopolymer concrete. *Materials & Design*, *44*, 580-586.

Shahmansouri, A. A., Nematzadeh, M., & Behnood, A. (2021). Mechanical properties of GGBFS-based geopolymer concrete incorporating natural zeolite and silica fume with an optimum design using response surface method. *Journal of Building Engineering*, *36*, 102138.

Siddique, R., Aggarwal, P., & Aggarwal, Y. (2011). Prediction of compressive strength of self-compacting concrete containing bottom ash using artificial neural networks. *Advances in engineering software*, *42*(10), 780-786.

Sujatha, T., Kannapiran, K., & Nagan, S. (2012). Strength assessment of heat cured geopolymer concrete slender column.

Sumajouw, M., & Rangan, B. V. (2006). Low-calcium fly ash-based geopolymer concrete: reinforced beams and columns.

Toufigh, V., & Jafari, A. (2021). Developing a comprehensive prediction model for compressive strength of fly ash-based geopolymer concrete (FAGC). *Construction and Building Materials*, *277*, 122241.

Verma, N. K., Meesala, C. R., & Kumar, S. (2023). Developing an ANN prediction model for compressive strength of fly ash-based geopolymer concrete with experimental investigation. *Neural Computing and Applications*, 1-17.

Vora, P. R., & Dave, U. V. (2013). Parametric studies on compressive strength of geopolymer concrete. *Procedia Engineering*, *51*, 210-219.